

Characteristics of a current sheet shear mode in collisionless magnetic reconnection

Keizo Fujimoto

Division of Theoretical Astronomy, National Astronomical Observatory of Japan
2-21-1 Ohsawa, Mitaka, Tokyo 181-8588, Japan

E-mail: keizo.fujimoto@nao.ac.jp

Abstract. The current study shows the characteristics of the kink-type electromagnetic mode excited in the thin current layer formed around the x-line during the quasi-steady phase of magnetic reconnection. The linear wave analyses are carried out for the realistic current sheet profile which differs significantly from the Harris current sheet. It is found that the peak growth rate is very sensitive to the current sheet width even though the relative drift velocity at the center of the current sheet is fixed. This indicates that the mode is excited by the velocity shear rather than the relative drift velocity. Thus, the mode is termed here a current sheet shear mode. It is also shown that the wavenumber k_y has a clear mass ratio dependency as $k_y \lambda_i \propto (m_i/m_e)^{1/4}$, implying the coupling of the ion and electron dynamics, where λ_i is the ion inertia length.

1. Introduction

Magnetic reconnection is a fundamental process in magnetized plasmas, generating fast plasma jets at the expense of the magnetic field energy. Although the process takes place in a microscopic region called the diffusion region formed around the magnetic x-line, the impact of the process extends over large distances beyond the kinetic scales from the x-line. Because of this multi-scale nature, it is believed that magnetic reconnection plays a significant role in large-scale dynamics of global phenomena such as geo-magnetospheric substorms and solar flares.

One of the main issues of magnetic reconnection is the mechanism breaking the frozen-in condition around the x-line and providing the large electric resistivity sufficient for a fast reconnection in collisionless plasmas. In two-dimensional (2D) reconnection, it has been demonstrated that the momentum transport due to the Speiser-type motion of the electrons gives rise to the electron viscosity around the x-line which leads to an effective resistivity [1, 2, 3, 4]. Although the electron viscosity gives sufficient dissipation for supporting the reconnection electric field under the thin current layer on the order of the electron inertia length, such a thin current sheet has not been observed neither in the laboratory experiments [5] nor in the geo-magnetosphere [6]. The observations have also shown intense activities of electromagnetic (EM) waves around the x-line [7]. The frequency range is usually from ω_{ci} to ω_{LH} , where ω_{ci} and ω_{LH} are the ion cyclotron frequency and the lower hybrid frequency, respectively. These observational facts imply the existence of the anomalous momentum transport due to the wave activities that are not incorporated in the 2D systems. In fact, kinetic simulations in three-dimensional (3D) system have revealed that kink-type EM waves are excited at the center of the current layer not only in the Harris sheet [8, 9, 10] but also in the thin current layer formed



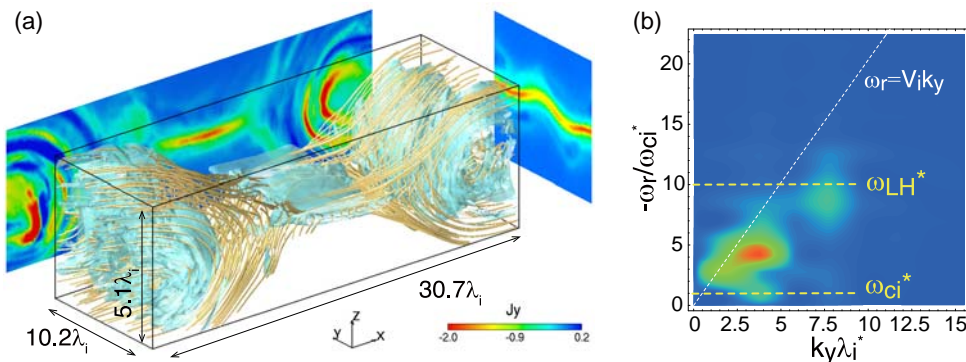


Figure 1. Simulation results. (a) 3D snapshot of an isosurface for $J_{xz} = \sqrt{J_x^2 + J_z^2} = 0.80 en_0 V_A$ with the magnetic field lines in yellow curves and 2D profiles of J_y at $x = 41.0\lambda_i$ (the center of the x system) and $y = 0.0$. (b) Wave spectrum of B_x at the dominant x-line averaged over the y axis during a fast reconnection. The phase velocity of V_{i0} is indicated by dotted curve in (b).

during a quasi-steady reconnection with anti-parallel configuration [11, 12]. These EM modes are important because they give the anomalous momentum transport and effective resistivity at the x-line. However, the generation mechanisms of the waves are poorly understood.

The linear properties of the waves responsible for the anomalous momentum transport have been investigated, so far, for the Harris-type current sheet [13, 10, 14]. In the Harris sheet, the pressure and current density gradients are supported by the density gradient with the uniform temperature and bulk velocity profiles [15]. Meanwhile, during the quasi-steady reconnection, the current sheet profile is far from the Harris sheet. For the case of symmetric reconnection, the density profile is almost uniform, so that the pressure and current density profiles are maintained through the temperature and bulk velocity gradients, respectively. Furthermore, the current sheet develops a two-scale structure consisting of the electron and ion current sheets. Therefore, it is very questionable that the previous results for the Harris sheet are still applicable in the quasi-steady phase of reconnection.

The purpose of this paper is to investigate the properties of the EM mode excited in the quasi-steady reconnection initiated with anti-parallel configuration. The linear wave analyses are employed for the realistic current sheet equilibrium based on the two-fluid equations. It is shown that the mode is excited due to the velocity shears rather than the relative drift velocity between the ion and electron. Thus, the mode is termed here a current sheet shear mode.

2. Simulation

The evidence of the kink-type EM mode has been recently reported in a large-scale particle-in-cell (PIC) simulation in 3D system [12]. Here we show an example of the simulation results. The simulation model employs adaptive mesh refinement (AMR) to achieve efficient multi-scale computation of magnetic reconnection [16]. The simulation is carried out for the Harris-type current sheet under the anti-parallel magnetic field configuration, which is common for magnetotail reconnection of the Earth. The domain size along the x-line is $L_y = 10.2\lambda_i$, where λ_i is the ion inertia length based on n_0 the number density at the center of the initial current sheet. The ion-to-electron mass ratio is $m_i/m_e = 100$. Magnetic reconnection is initiated with a small perturbation to the magnetic field B_x and B_z , which produces the x-line at the center of the xz domain. More detailed setup is described in Fujimoto and Sydora [12].

Figure 1a shows a snapshot of the 3D current layer during a quasi-steady fast reconnection. It is evident that a kink mode is excited in the electron current layer formed around the x-line. The

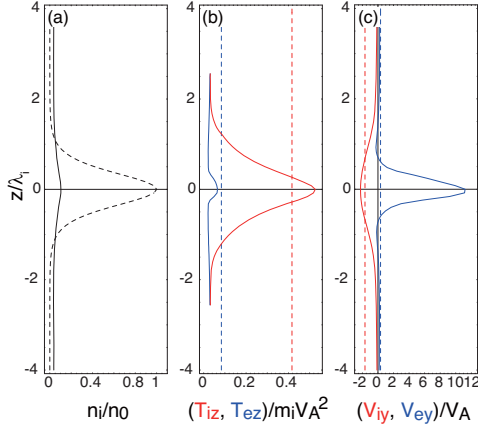


Figure 2. 1D profiles averaged over the y axis at the dominant x -line in the simulation for (a) ion density, (b) ion (red curves) and electron (blue curves) temperatures, and (c) ion (red curves) and electron (blue curves) out-of-plane bulk velocities. The solid and dashed curves indicate the profiles during a fast reconnection and of the Harris current sheet, respectively.

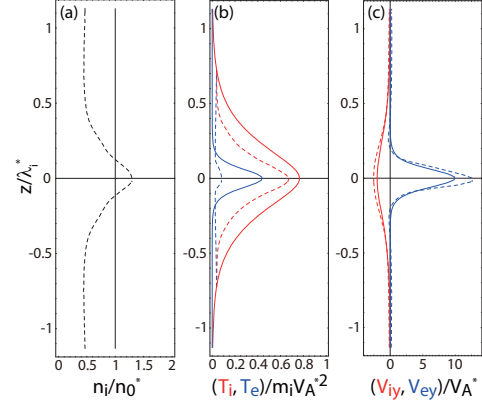


Figure 3. Example of the model current sheet (solid curves) used for the linear analyses of (a) number density, (b) ion (red curves) and electron (blue curves) temperatures, and (c) ion (red curves) and electron (blue curves) out-of-plane bulk velocities. The dashed curves indicate the profiles during a fast reconnection.

mode is an EM mode and propagates in the y direction (i.e., current density direction) almost with the ion flow velocity V_{iy} . The wave spectrum in the ω - k_y space (Fig. 1b) reveals that the mode has a frequency between ω_{ci}^* and ω_{LH}^* , consistent with the observations [7], where the asterisk indicates the local values. As discussed in the previous paper [12], this mode provides the anomalous resistivity at the x -line, so that the understanding of the wave characteristics is very important in reconnection physics.

3. Linear analysis

Most of the previous linear analyses of the kink-type EM modes have been carried out for the Harris current sheet [13, 10, 14]. As shown in Fig. 2 (dashed curves), the Harris sheet is characterized by the non-uniform density profile with the uniform temperature and bulk velocity profiles to make the pressure and current density gradients. However, these profiles are drastically changed after the onset of the fast reconnection. During the quasi-steady phase of reconnection, the density is almost uniform across the current sheet, and the pressure and current density gradients are generated due to the non-uniform temperature and bulk velocity profiles (see solid curves in Fig. 2). Therefore, it is very questionable that the previous results for the Harris sheet are still applicable in the quasi-steady reconnection. In fact, since there is little density gradient, the lower hybrid drift instability [14] is hardly excited in this current layer.

In the present study, a more realistic equilibrium is introduced to mimic the current sheet profiles during the quasi-steady reconnection. The new equilibrium is based on the two-fluid equations, and is provided by the following relations:

$$n_i(z) = n_e(z) = \text{const.}, \quad (1)$$

$$B_x(z) = B_{0i} \tanh(z/\delta_i) + B_{0e} \tanh(z/\delta_e), \quad (2)$$

$$V_s(z) = -V_{s0}/\cosh^2(z/\delta_s), \text{ and} \quad (3)$$

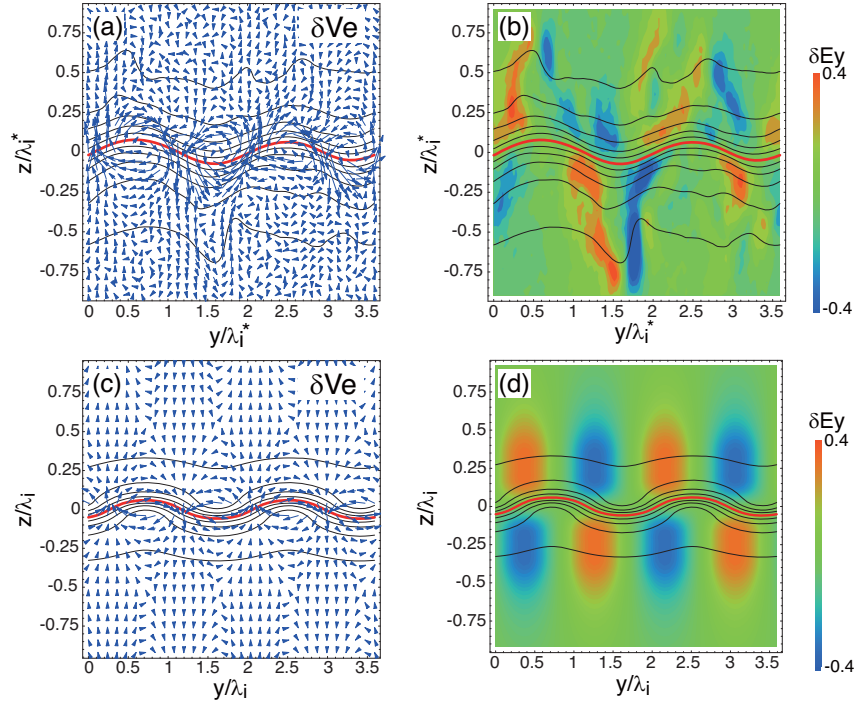


Figure 4. (a, b) Simulation results in the yz plane through the dominant x -line of (a) $\delta\vec{V}_e$ (arrows) the deviation of the electron bulk velocity from the values averaged over the y axis at each z location and (b) δE_y (color contours) the deviation of E_y . (c, d) Eigenfunctions solved through the theoretical linear analyses of (c) $\delta\vec{V}_e$ (vectors) and (d) δE_y (color contours). The black curves represent the contours of B_x , and the red curves show the contours at $B_x = 0$.

$$T_s(z) = - \int^z q_s V_s(\xi) B_x(\xi) d\xi, \quad (4)$$

where s indicates the species and there must be the relation $V_{s0} = (1/\mu_0 n q_s)(B_{0s}/\delta_s)$ to satisfy the Ampère's law. In Fig. 3, an example of the equilibrium profiles is shown for the case of $B_{0i}/B_0^* = 2.0$, $B_{0e}/B_0^* = 1.0$, $\delta_i/\lambda_i^* = 0.35$, $\delta_e/\lambda_e^* = 1.0$, and $m_i/m_e = 100$, where B_0^* is assumed to be the magnetic field at the inflow edge of the electron diffusion region. One can see that the profiles in the simulation (dashed curves) are reproduced in the model current sheet, providing the two-scale structure with the temperature and bulk velocity gradients. The wave dispersion is obtained by solving the linearized two-fluid equations for $\omega = \omega_r + i\gamma$ numerically using an initial value approach starting with small random noise [13].

In Fig. 4, the simulation results and the eigenfunctions obtained by the linear analyses are compared for $\delta\vec{V}_e$ and δE_y , where δA in the simulation is calculated by $\delta A \equiv A - \langle A \rangle_y$ with $\langle \cdot \rangle_y = \int_0^{L_y} \cdot dy / L_y$. The current sheet structure predicted by the linear analyses is well consistent with the simulation results, regarding the kinked structure, electric field structure, and the associated electron flow structure. We have also confirmed that the dispersion relation in the ω - k_y space matches the simulation result in Fig. 1b. These consistencies demonstrate that the two-fluid approximation is valid for this EM mode.

To investigate further the characteristics of the wave, we calculate the δ_i dependency of the peak growth rate. It is important to note that the peak bulk velocities V_{i0} and V_{e0} are fixed in this analysis. Therefore, the relative drift velocity between the species is not changed at the center of the current layer. As shown in Fig. 5a, the peak growth rate is drastically

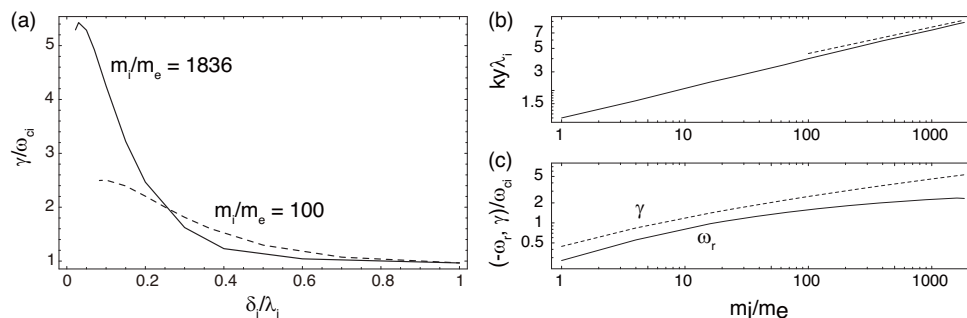


Figure 5. Theoretical linear properties of the electromagnetic wave. (a) Dependency of the growth rate γ on the width of the ion current sheet δ_i for the cases of $m_i/m_e = 100$ (dashed curves) and $m_i/m_e = 1836$ (solid curves). (b, c) Dependencies on m_i/m_e of (b) the wavenumber k_y and (c) the real frequency ω_r (solid curve) and growth rate γ (dashed curve). The dashed curve in (b) indicates the relation $k_y\lambda_i = \sqrt{2}(m_i/m_e)^{1/4}$.

decreased as δ_i the width of the ion current layer increases for both the cases of $m_i/m_e = 100$ and $m_i/m_e = 1836$, where $\delta_e = \lambda_e^*$ is assumed in each mass ratio. This indicates that the mode is very sensitive to the velocity shear rather than the relative drift velocity, implying that the mode is driven by the velocity shear. The wave characteristics differs from that of the drift kink mode, where the peak growth rate depends on the relative drift velocity as $\gamma \propto |V_{i0} - V_{e0}|$ [13].

We next consider the dependency on m_i/m_e the ion-to-electron mass ratio, assuming $\delta_i = \delta_e = \lambda_e^*$. As displayed in Figs. 5b and 5c, the EM mode has a clear m_i/m_e dependency in spatio-temporal scales. In particular, it is found that the wavenumber k_y has a relation of $k_y\lambda_i^* \simeq \sqrt{2}(m_i/m_e)^{1/4}$, so that the wavelength is scaled with $\lambda \propto \sqrt{\lambda_i^*\lambda_e^*}$ an intermediate scale between the ion and electron scales. The peak growth rate increases as m_i/m_e increases. This is because the current sheet width (shear scale) decreases and the peak velocity increases with the mass ratio. Even though the width of the ion current layer δ_i is larger than λ_e^* , the asymptotic value of γ is comparable between the cases of $m_i/m_e = 100$ and 1836 (Fig. 5a). Thus, the mode survives even in the realistic mass ratio. The clear m_i/m_e dependency suggests that the mode differs from the ion-ion kink mode, where the spatio-temporal scales are determined only by the ion physics [10].

4. Summary

The current study has investigated the characteristics of the kink-type EM mode excited in the electron current layer formed around the x-line during the quasi-steady phase of magnetic reconnection. The mode is important in reconnection physics because it is known to provide the anomalous resistivity at the x-line. The linear wave analyses are carried out for the realistic current sheet which differs significantly from the Harris current sheet. The new equilibrium current sheet consists of two-scale structure of the ion and electron current sheets. The pressure and current density gradients are supported by the temperature and bulk velocity gradients, respectively, with uniform number density. The wave dispersion was gained by solving the linearized two-fluid equations numerically.

We first confirmed that the eigenfunctions obtained in the linear analyses are consistent with the simulation results, which warrants the two-fluid approximation for this mode. Further analyses revealed that the peak growth rate decreases drastically as the current sheet width increases, even though the relative drift velocity is fixed at the center of the current layer. Thus, it is reasonable to conclude that the mode is driven by the velocity shears rather than the relative

drift velocity, so that the mode is termed here a current sheet shear mode. We also found that the mode has a clear mass ratio dependency of $k_y \lambda_i \propto (m_i/m_e)^{1/4}$, implying the coupling of the ion and electron dynamics.

Since the current linear analyses employ the numerical approach, the theoretical background behind the mass ratio dependency is not completely understood. The analytical analysis is needed in near future to clarify more the generation mechanism of the current sheet shear mode.

Acknowledgments

The simulations were carried out by Fujitsu FX1 installed at the ITC, Nagoya University, with support from the HPC joint research project at Nagoya University and a computational joint research program at the STE Laboratory, Nagoya University.

References

- [1] Speiser T W 1970 *Planet. Space Sci.* **18** 613–22
- [2] Cai H J and Lee L C 1997 *Phys. Plasmas* **4** 509–20
- [3] Hesse M, Schindler K, Birn J and Kuznetsova M 1999 *Phys. Plasmas* **6** 1781–95
- [4] Fujimoto K and Sydora R D 2009 *Phys. Plasmas* **16** 112309
- [5] Ji H, Ren Y, Yamada M, Dorfman S, Daughton W and Gerhardt S P 2008 *Geophys. Res. Lett.* **35** L13106
- [6] Wygant J R *et al* 2005 *J. Geophys. Res.* **110** A09206
- [7] Zhou M *et al* 2009 *J. Geophys. Res.* **114** A02216
- [8] Zhu Z and Winglee R M 1996 *J. Geophys. Res.* **101** 4885–97
- [9] Horiuchi R and Sato T 1999 *Phys. Plasmas* **6** 4565–74
- [10] Karimabadi H, Daughton W, Pritchett P L and Krauss-Varban D 2003 *J. Geophys. Res.* **108** 1400
- [11] Fujimoto K 2009 *Phys. Plasmas* **16** 042103
- [12] Fujimoto K and Sydora R D 2012 *Phys. Rev. Lett.* **209** 265004
- [13] Pritchett P L, Coroniti F V and Decyk V K 1996 *J. Geophys. Res.* **101** 27413–29
- [14] Daughton W 2003 *Phys. Plasmas* **10** 3103–19
- [15] Harris E G 1962 *Nuovo Cimento* **23** 115–21
- [16] Fujimoto K 2011 *J. Comput. Phys.* **230** 8508–26